Optical forces due to spherical microresonators and their manifestation in optically induced orbital motion of nanoparticles

J. T. Rubin and L. I. Deych
Department of Physics, Queens College of the City University of New York, Flushing, New York 11367, USA and The Graduate School and University Center, The City University of New York, 365 Fifth Avenue, New York, New York 10016, USA

(Received 28 December 2010; revised manuscript received 21 July 2011; published 26 August 2011)

By considering the interaction between whispering-gallery modes of a spherical resonator and a subwavelength polarizable particle, we demonstrate that spatial confinement of the electromagnetic field dramatically changes the character of the optical forces exerted. We show that this phenomenon can be experimentally observed in the optically induced orbital motion of the particle.

DOI: 10.1103/PhysRevA.84.023844 PACS number(s): 42.79.Gn, 37.10.Mn

I. INTRODUCTION

Since the early work of Ashkin on optical trapping with focused laser beams [1], particle manipulation by optical forces has become a standard tool in atomic physics, biology, and medicine. Optical forces are usually separated into two components: the conservative "gradient" force, which in the dipole approximation is proportional to the real part of the particle's complex polarizability α, and a nonconservative "scattering" force, which is proportional to its imaginary part [2]. Recently, a great deal of attention has been focused on optical trapping of small dielectric particles using the modes of optical cavities [3–8], both for classical applications [3–5] and for fundamental studies in the field of quantum optomechanics [6–8]. In the latter case, an established paradigm is based on the assumption that the "gradient" component of the optical force remains conservative even when the electromagnetic field is confined within a cavity, and, therefore, can be characterized by a potential. This potential in the dipole approximation is expressed in terms of the particle-induced shift of the cavity resonance [6–8]. However, the thermodynamic arguments relating the optical force on a dipole to the effective potential are specifically based on the assumption that the dipole introduced into a field does not affect the distribution of charges or currents producing it [9]. This assumption fails in the case of a particle interacting with cavity modes because the distribution of the charges on the cavity walls depends on the position of the particle. The consequences of this dependence are much deeper than a simple change of the cavity's resonance frequency. We will show here that in this case the gradient component of the optical force, defined by its dependence on Re[α], becomes nonconservative, which has obvious implications for the quantum theory of optomechanical interaction in the cavities [7,8,10].

The first demonstration of the difficulties of the traditional approach to optical forces in optical resonators was given in Ref. [4], where it was shown that direct computation of the gradient of the particle's potential energy due to its interaction with the *one-dimensional* cavity field results in spurious terms. However, the cavity-induced modification of the optical force has even more profound consequences in situations where the particle's motion is fully *three dimensional*. Such a situation was, for instance, observed in Ref. [3] and subsequent works [11,12], where a nanoparticle suspended in a solution was set into orbital motion around a whispering-gallery mode (WGM) resonator. The driving torque responsible for sustaining the particle in orbit is clearly nonconservative and was presumed to be of scattering origin [3]. However, we show here that this torque has a contribution proportional to Re[α], which is not related to the scattering force.

The orbital motion observed in Refs. [3], [11], and [12], besides being a manifestation of the nontrivial effect of the cavity on optical forces, is of interest in its own right. Unlike more traditional optomechanical systems, where mechanical motion is effectively one dimensional (see reviews [10,13]), this situation involves long-range displacement of the particle with optically induced coupling between all three mechanical degrees of freedom. Therefore this phenomenon introduces a wide array of previously unexplored optomechanical phenomena.

In this paper, we pursue three main goals. First, using the interaction of a particle with WGMs of a spherical resonator as an example, we demonstrate the profound consequences that cavity confinement has on optical forces. Second, we develop an *ab initio* theory of the optically induced orbital motion, and finally, we identify experimental manifestations of the predicted cavity effects, and establish conditions required for their observation.

II. INTERACTION BETWEEN A WGM AND A SUB-WAVELENGTH PARTICLE

In our calculations we use representation of the electromagnetic field of a spherical dielectric cavity (radius R_s, refractive index n_s) in terms of the vector spherical harmonics (VSHs), characterized by polar l and azimuthal m indexes, as well as polarization (E or M modes). For each l, there are $2l+1$ degenerate m modes with frequency $\omega_{l,s}^{(0)}$ and radiative decay rate $\Gamma_{l,s}^{(0)}$. The index s distinguishes resonances with different radial behavior. Modes with $|m| = l \gg 1$, $s = 1$ are localized near $r = R_s$, $\theta = \pi/2$ and are known as fundamental WGMs. Since in this paper we only consider modes with $s = 1$, this index will be omitted in what follows.

A subwavelength dielectric particle of radius R_p, refractive index n, and mass M_p introduced into the evanescent field of the resonator modifies its spectrum [14–16], giving rise, in addition to $\omega_l^{(0)}$, to one (TE) or two (TM) resonances [15,16]. This effect is best understood by switching from the traditional coordinate system with its polar axis perpendicular to the

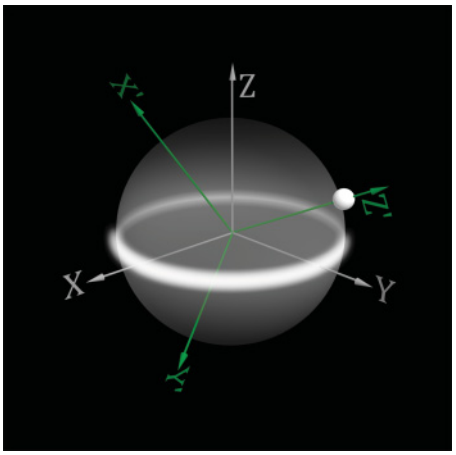

FIG. 1. (Color online) Schematic representation of the resonator, particle, WGM, and two coordinate systems.

plane of the fundamental WGM (XYZ system in Fig. 1) to the rotated systems ($X'Y'Z'$ in Fig. 1) and $\tilde{X}\tilde{Y}Z'$ (not shown), whose polar axes pass through the centers of the resonator and the particle, and which are centered at the resonator and the particle, respectively. The single VSH, describing the field of the unmodified (in the absence of the particle) fundamental WGM with polar number L, becomes a linear combination of VSHs defined in the $X'Y'Z'$ system. The field scattered by the particle in the $\tilde{X}\tilde{Y}Z'$ system is described in the dipole approximation by the $l = 1$ mode with $m' = 0, \pm 1$. Since the translation of these modes along the Z' axis does not affect their m decomposition, the particle interacts only with $m' = -1,0,1$ modes of the resonator, shifting their resonance frequencies. The remaining $2L - 2$ resonator modes with $|m'| > 1$ are completely unaffected by the particle and resonate at $\omega_L^{(0)}$. The modes $m' = \pm 1$ are degenerate and resonate at frequency $\omega_p = \omega_L^{(0)} + \delta\omega_L$ with width $\Gamma_p = \Gamma_L^{(0)} + \delta\Gamma_L$ (explicit expressions for $\delta\omega$ and $\delta\Gamma$ can be found in Refs. [15,16]). For TM polarized WGMs, the $m' = 0$ mode has an additional resonance, while for TE modes, this mode is unaffected by the particle and resonates at $\omega_L^{(0)}$.

This qualitative picture of the sphere-particle interaction is verified by an explicit *ab initio* calculation of the field distribution and resonances of the coupled resonator-particle system, which in the dipole approximation can be presented in closed analytical form [15,16]. Details of these calculations are given in the Appendix. By using rigorous expressions for the electric and magnetic fields obtained in Refs. [15,16], one can compute optical forces on the stationary particle from the Maxwell stress tensor. The extension of these results to the case of a slowly moving particle is possible if the mechanical time scale is much longer than the relaxation time of the resonator $Q/\omega_L^{(0)}$ (so-called unresolved sideband regime) [10]. We demonstrate below that for a large range of experimental parameters, this is indeed the case.

III. OPTICAL FORCE ON THE PARTICLE

The time-averaged force exerted by the electromagnetic field on a spherical region V bounded by surface S is obtained by integration of the Maxwell stress tensor $\overleftrightarrow{\mathbf{T}}$:

$$\mathbf{F} = \oint_S \overleftrightarrow{\mathbf{T}} \cdot d\mathbf{a}, \tag{1}$$

where

$$\overleftrightarrow{\mathbf{T}} = \frac{n_0}{2}\mathrm{Re}\left\{\epsilon_0 \mathbf{E}^*\mathbf{E} + \mu_0 \mathbf{H}^*\mathbf{H} - \frac{1}{2}(\epsilon_0|E|^2 + \mu_0|H|^2)\ \overleftrightarrow{\mathbf{I}}\right\}. \tag{2}$$

The unit dyadic $\overleftrightarrow{\mathbf{I}} = \hat{\mathbf{x}}\hat{\mathbf{x}} + \hat{\mathbf{y}}\hat{\mathbf{y}} + \hat{\mathbf{z}}\hat{\mathbf{z}}$, and $\hat{\mathbf{x}},\hat{\mathbf{y}},\hat{\mathbf{z}}$, are the Cartesian unit vectors.

For a field represented as an expansion in VSHs, the integral in Eq. (1) can be presented explicitly in terms of the VSH expansion coefficients [17]. We employ several approximations to simplify the result. Coupling to the particle excites VSHs in the resonator with different polar numbers $l \neq L$ and different polarizations [15,16]. However, if $\omega_{L+1}^{(0)} - \omega_L^{(0)} \gg \delta\omega_L$, we can introduce the resonant approximation (RA), in which forces are calculated neglecting these modes in the VSH expansion. Additionally, rather than performing the integration over a surface surrounding the particle, we use a surface surrounding the resonator and appeal to Newton's third law to find the force on the particle. The validity of this procedure is confirmed by calculation of the stress tensor integral over a surface surrounding the resonator and particle, which vanishes in the RA.

When the system is near one of the particle-induced resonances, and $|\delta\omega_L| \gg \Gamma_p$, one can also introduce the reduced resonance approximation (RRA) by retaining in the VSH expansion only terms with $m' = \pm 1$. The RRA will be used later for comparison to the RA results.

We assume that the microsphere is excited by a steady-state signal with constant frequency ω offset from the frequency of the ideal WGM resonance of mode L: $\omega = \omega_L^{(0)} + \Delta$. The relative detuning from the induced resonance depends only on the distance r_p between the centers of the resonator and particle, $y(r_p) = (\omega - \omega_p)/\Gamma_p \equiv (\Delta - \delta\omega_L)/\Gamma_p$. Coupling is maximized when $y = 0$, that is, when the particle occupies a position $r_p = r_0$ such that the induced resonance occurs at the driving frequency of the system, $\omega_p(r_0) = \omega$. Since $\delta\omega_L < 0$ for particles surrounded by an optically less-dense medium, the nominal detuning Δ must be negative to satisfy this condition. By keeping only terms linear in the particle's polarizability, and assuming $\Delta/\Gamma_L^{(0)} = \kappa^{-1} > 1$, the force can be presented as

$$\mathbf{F} = F_r\hat{r} + F_\phi\hat{\phi} + F_\theta\hat{\theta} = -f_0\mathcal{A}[\hat{\mathbf{r}} + (g\kappa)(\hat{\phi} + y\bar{\theta}\hat{\theta})], \tag{3}$$

where $\bar{\theta}$ is the deviation of the particle's polar coordinate θ_p from $\pi/2$: $\bar{\theta} = \theta_p - \pi/2$, $\hat{r}$, $\hat{\phi}$. $\hat{\theta}$ are radial, azimuthal, and polar unit vectors in the XYZ coordinate system, while dimensionless amplitude $\mathcal{A}(y,\bar{\theta}) = e^{-L\bar{\theta}^2}/(y^2 + 1)$, and f_0 is given by

$$f_0 = \frac{\mathrm{Re}[\alpha]|E_0|^2}{12\pi}\left(\frac{\Gamma_L^{(0)}}{\Gamma_p}\right)^2 \frac{U_{L,1,\sigma}}{\sqrt{\pi L}}(U_{L-1,1,\sigma} - U_{L+1,1,\sigma}). \tag{4}$$

Here E_0 is the amplitude normalization factor, which can be related to the power radiated by a WGM, and $U_{l,1,\sigma}$ are translation coefficients describing coupling between the field of a dipole and the WGM of the resonator with polar number l and given polarization, which are given explicitly in the

Appendix. Parameter g is of the order of unity and depends on the polarization of the initial WGM of the resonator. If this mode is of the magnetic type, we have

$$g_M = \frac{\Gamma_p}{\Gamma_L^{(0)}} \frac{U_{L-1,1,M} + U_{L+1,1,M}}{U_{L-1,1,M} - U_{L+1,1,M}}, \tag{5}$$

while for the electric modes, the contribution of the additional resonance with $m = 0$ modifies this expression to

$$g_E = \frac{\Gamma_p}{\Gamma_L^{(0)}} (U_{L-1,1,E} - U_{L+1,1,E})^{-1} \Bigg[(U_{L-1,1,E} + U_{L+1,1,E}) \times \left(1 + \frac{\Delta}{\Delta_E}\right) + \frac{\Delta}{\Delta_E} \frac{U_{L,0,E}}{U_{L,1,E}} U_{L-1,0,E} + U_{L+1,0,E} \Bigg], \tag{6}$$

where $\Delta = \omega - \omega_L^{(0)}$ and

$$\Delta_E = \omega - \Gamma_L^{(0)} \frac{\mathrm{Re}\alpha [U_{L,0,E}]^2}{6\pi\epsilon_0}.$$

Figure 2 presents a color plot of the forces for an initial WGM of the electric type, which shows resonant dependence of the force upon azimuthal and radial coordinates with two resonances corresponding to $|m| = 1$ ($y = 0$) and $m = 0$ ($y \approx 40$) particle-induced frequencies. One can see from this figure that nonoverlapping spectral resonances indeed yield well-separated spatial resonances.

In order to relate the obtained results with phenomenological description of optomechanical interaction we replace the RA field with its RRA approximation. In this case the azimuthal and polar components of the force vanish while remaining radial component can be presented as follows.

Making use of the recursion relation for Hankel functions, one can show that in the large L limit (neglecting $1/L$ terms), the translation coefficients obey the following recursion relations:

$$2U'_{lm\sigma} = U_{l-1,m,\sigma} - U_{l+1,m,\sigma},$$

where the prime denotes differentiation with respect to argument. Comparing this result with Eq. (A12), one can see that f_0 may be written as

$$f_0 = \frac{\epsilon_0 |E_0|^2}{2k^3\sqrt{\pi L}} \left(\frac{\Gamma_L^{(0)}}{\Gamma_p}\right)^2 \frac{1}{\Gamma_L^{(0)}} \frac{d\delta\omega_L}{dr_p}. \tag{7}$$

To further elucidate the meaning of this expression, we introduce the power radiated from the resonator, $P = \oint_S \mathbf{S} \cdot d\mathbf{a}$, where $\mathbf{S} = \mathbf{E} \times \mathbf{H}$, which is given by

$$P = \frac{\epsilon_0 c^3}{2\omega^2} \sum_{m,l,\sigma} |C_{lm\sigma}|^2.$$

In the RRA, this becomes

$$P \approx \frac{\epsilon_0 c^3 |E_0|^2}{\omega^2 \sqrt{\pi L}} \left(\frac{\Gamma_L^{(0)}}{\Gamma_p}\right)^2 \mathcal{A} \equiv P_0 \mathcal{A}, \tag{8}$$

where P_0 is the power emitted by the resonator in the RRA approximation at exact resonance. Now, defining the average photon number as

$$N = \mathcal{A} \frac{P_0 [2\Gamma_L^{(0)}]^{-1}}{\hbar\omega},$$

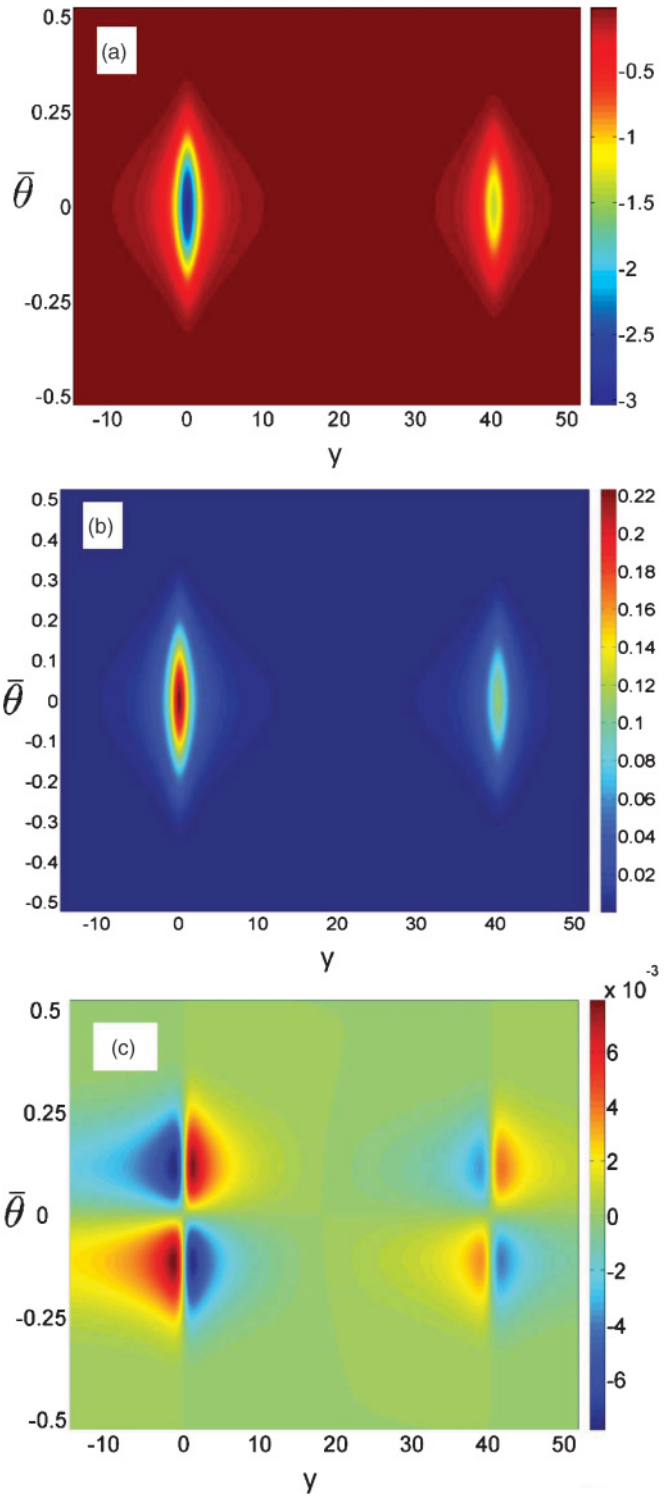

FIG. 2. (Color online) Vector components of the optical force in units of $\epsilon_0 |E_0|^2/k^2$. (a) F_r, (b) F_ϕ, (c) F_θ, for $L = 39$, E-type mode, $R_p/R_s = 0.01$, $n = 1.59$, and $\kappa^{-1} = 100$.

where the factor of 2 is introduced to define the lifetime of intensity of the resonator mode, rather than of its amplitude, one can present F_r^{RRA} as

$$F_r^{\mathrm{RRA}} = -f_0 \mathcal{A} = -N\hbar \frac{d\delta\omega_L}{dr_p}. \tag{9}$$

Using the classical analog of a commonly employed, optomechanical Hamiltonian $H = \hbar\delta\omega\hat{a}^\dagger\hat{a}$ [6,7], where $\hat{a}^\dagger$ and $\hat{a}$ are photon creation-annihilation operators ($\hat{a}^\dagger\hat{a} \to \langle\hat{a}^\dagger\hat{a}\rangle = N$), to calculate the force, one would obtain $F \propto \partial(N\delta\omega)/\partial r_p$. Since in cavities under steady-state illumination conditions N depends on the particle's position, this result is not equivalent to the $F_r^{(\mathrm{RRA})}$ derived in this paper. The difference between the two expressions is significant even in high-Q cavities, as was demonstrated recently in Ref. [4].

Azimuthal and polar components of the force in Eq. (3) can only be obtained by going outside of RRA. Physically it means that while the radial component of the force can be explained purely by the particle-induced frequency shift of the resonator, the other two components are due to the particle-induced change of the spatial configuration of the field. In the case $\kappa^{-1} > 1$ considered here, the largest contribution to the azimuthal and polar components of the force in Eq. (3) is proportional to $\mathrm{Re}[\alpha]$, and is not related, therefore, to the scattering portion of the force. While originating from what is usually thought of as the gradient force, the azimuthal component of the force in Eq. (3) is clearly nonconservative, reflecting fundamental change in the nature of the optical forces brought about by the field confinement in the cavity.

IV. PARTICLE DYNAMICS

It is convenient to analyze particle dynamics by introducing dimensionless time $\tau = t/T$ and angular momentum $\zeta = M_p r_p^2\dot{\phi}\cos\bar{\theta}/\Lambda$, where $T = \sqrt{M_p r_0/f_0}$ and $\Lambda = \sqrt{M_p r_0^3 f_0}$. The detuning y, linearized about zero, can be used as a dimensionless radial coordinate of the particle, $y = (r_p - r_0)y'(r_0)$ (prime denoting differentiation with respect to r_p), with $1/y'(r_0)$ playing the role of a spatial width of the mode. It is inversely proportional to f_0 and is characterized by a dimensionless parameter $b = [y'(r_0)r_0]^{-1}$. Using asymptotic expansions for the Hankel functions, one can show that $b = O(\kappa/L) \ll 1$.

To the first order in $\bar{\theta}$ and its time derivatives, the equations of motion for the particle take the form of

$$\frac{d^2y}{d\tau^2} = \frac{\zeta^2}{b} - \frac{1}{b(y^2+1)}, \tag{10}$$

$$\frac{d\zeta}{d\tau} = -\frac{\kappa g}{y^2+1}; \quad \frac{d^2\bar{\theta}}{d\tau^2} = -\left(\zeta^2 + \frac{\kappa g y}{y^2+1}\right)\bar{\theta}, \tag{11}$$

where the terms proportional to ζ^2 are of the usual kinematic origin. Time and orbital momentum scales T and Λ correspond to the period and angular momentum for the circular orbit of radius r_0 in the $\bar{\theta} = 0$ plane in the absence of the azimuthal component of the optical force. The increase of ζ ($\kappa < 0$) over this time scale $\Delta\tau = 1$ is $d\zeta/d\tau \approx |\kappa|g < 1$, which shows that the angular momentum changes slowly over the orbital time scale. In this case, the radial motion, described by Eq. (10), occurs in an effective, slowly changing potential characterized by a stable equilibrium $y_0 = -\sqrt{\zeta^{-2} - 1}$, which exists for $\zeta < 1$. However, if the angular velocity is too small, the particle crashes on the surface of the resonator. Taking these two limitations into account, one obtains that the radial motion of the particle can be trapped by the resonator if $\zeta_{\min} < \zeta < 1$, where $\zeta_{\min} = \{[(r_0 - R_s)/(br_0)]^2 + 1\}^{-1/2}$. In this case, the radial motion can be approximately described as harmonic oscillations with adiabatically time-dependent frequency $\Omega_r = \zeta^2(-2y_0/b)^{1/2} > 1$. When the particle deviates from the $\bar{\theta} = 0$ plane, second-order terms in the $\bar{\theta}$ coordinate [neglected in Eqs. (10) and (11)] arising from the factor $e^{-L\bar{\theta}^2}$ in the force in Eq. (3) can play a role since $L \gg 1$. For constant y, Eq. (11) describes harmonic oscillations about $\bar{\theta} = 0$ with frequency $\Omega_\theta \approx |\zeta| \ll \Omega_r$. Therefore, the effect of the polar dynamics on the radial coordinate can be described by replacing the expression for the equilibrium with $y_0 \to -\sqrt{y_0^2 - L\bar{\theta}^2/\zeta^2}$. This point oscillates with $\bar{\theta}$ over the time scale $\tau_\theta = 2\pi/\Omega_\theta$, while increasing overall due to the increase in ζ.

Even though the presence of a nonconservative azimuthal force makes the dynamics of the particle non-Hamiltonian, qualitatively its radial dynamics can be understood by considering it as occurring in an adiabatically changing, effective potential

$$u_{\mathrm{eff}} = (-\zeta^2 y + \arctan y)/b - (L\bar{\theta}^2/b)\arctan y,$$

with quasienergy

$$\epsilon = (d\bar{y}/d\tau)^2/2 + u_{\mathrm{eff}}.$$

Assuming for simplicity $\bar{\theta} = 0$, we find that this potential allows for two equilibrium points at $y_{\max,\min} = \pm\sqrt{1/\zeta^2 - 1}$, with the one with negative sign corresponding to the stable equilibrium. The plot of this potential for several values of ζ is shown in Fig. 3. The depth of the potential can be estimated as $U_{\mathrm{rad}} \equiv u_{\mathrm{eff}}(y_{\max}) - u_{\mathrm{eff}}(y_{\min}) \sim \arctan(y_{\min})/b$, which, after translation to the physical variables, produces the expression

$$U_{\mathrm{rad}} \approx (\Lambda_0/T)\arctan(\sqrt{1-\zeta^2}/\zeta).$$

The analysis provided above is possible because of the clear separation of time scales between orbital, polar, and radial degrees of freedom, with the latter being the fastest. Therefore, radial frequency Ω_r sets up limits of applicability of the unresolved sideband approximation, which can now be formulated as $\Omega_r \ll T\Gamma_p$. In terms of external parameters, this inequality can be rewritten in the form of the lower

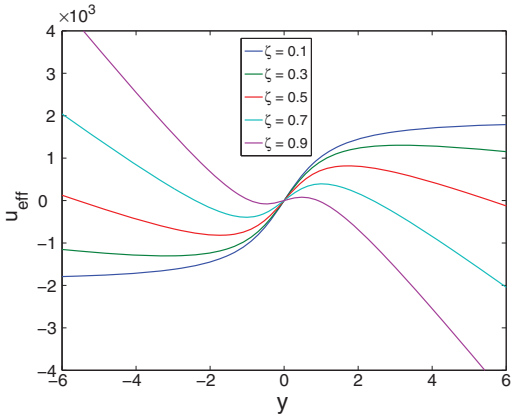

FIG. 3. (Color online) The shape of the effective potential for $\bar{\theta} = 0$ and several values of angular momentum ζ. One can see how the potential well disappears when ζ approaches unity.

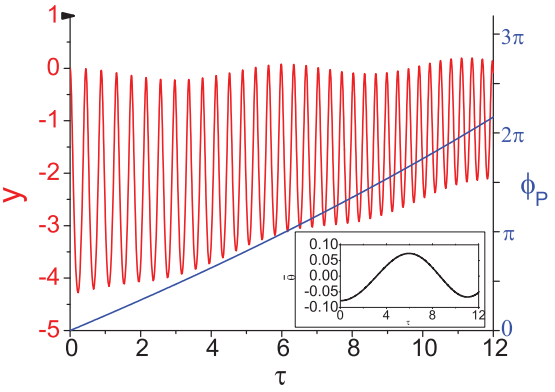

FIG. 4. (Color online) Time dependence of particle coordinates computed for the same parameters as in Fig. 2 with initial conditions $y = 0, \zeta = .4$, and $\bar{\theta} = 0.08$. The rapidly oscillating curve represents the radial coordinate, the monotone line in the main figure shows the azimuthal coordinate, and the inset shows the polar coordinate.

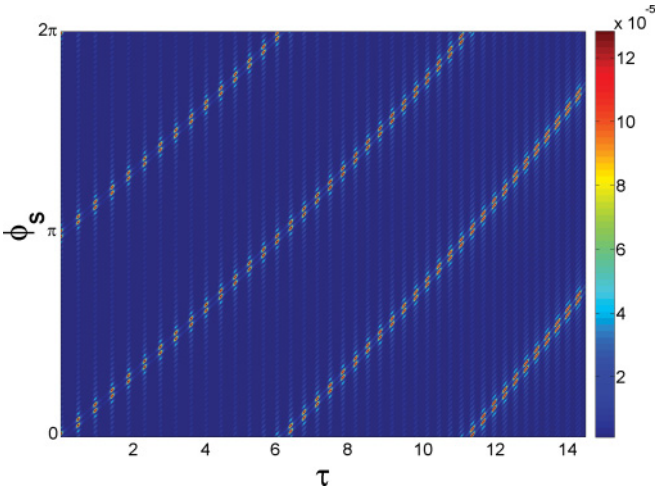

FIG. 5. (Color online) Color map of the field intensity of the resonator at $\theta = \pi/2$ and $0 < \phi_s < 2\pi$ as a function of time. Brighter tones correspond to larger intensity of the field.

limit on the mass of the particle: $M_p \gg P/(\Gamma_p r_0^2 b^2 \omega^2)$. For instance, if $R_p = 100$ nm, $R_s = 50\ \mu$m, $P = 50\ \mu$W, and $\omega = 3 \times 10^{14}$ Hz, which are typical values for experiments of this kind [3,6], we obtain that quasistatic approximation for the field is valid for particles with $M_p \gg 10^{-16} g$. The minimum value of the orbital momentum allowing for the particle to orbit the resonator in this case is $\zeta_{\min} \approx 0.12$. A particle with $M_p = 10^{-13} g$, similar to those used in Ref. [3], will be trapped by the radial quasipotential if its linear velocity v is in the range $10 < v < 100$ cm/s. Numerical simulations of the particle trajectories (Fig. 4) show that if the initial velocity of the particle is close enough to its minimum value, then the particle will undergo at least one complete revolution before its tangential velocity reaches the upper critical value.

To estimate the feasibility of experimental verification of the predicted properties of the optical force, one has to take into account effects due to the particle's environment, such as thermal fluctuations and a viscous force $\mathbf{F_v} = -M_p \beta d\mathbf{r}_p/dt$. The latter limits the particle's angular momentum to its terminal value $\zeta_{\text{term}} \propto \kappa/(\beta T)$, which is reached in time $\tau_{\text{term}} \propto (\beta T)^{-1}$. If $\zeta_{\text{term}} \gg 1$, which also implies $\tau_{\text{term}} \gg 1$, then the effect of the drag force can be neglected. However, if $\zeta_{\min} < \zeta_{\text{term}} < 1$, which ensures the existence of the radial potential well, then the drag force can actually play a positive role in stabilizing the particle's motion against run-away growth of the orbital momentum. For particles with the same parameters as above and in air at normal pressure, $\beta T \approx 1$. Thus, in order to achieve the stable orbital motion of the particles, one needs to place the particle in a moderately rarefied atmosphere with densities just two orders of magnitude less than the ambient value. The initial and/or terminal values of ζ must also be small enough to ensure sufficient depth of the radial potential U_{rad} compared to the thermal energy. For the same parameter as before, the former can be estimated as $U_{\text{rad}} \sim 10^{-17} J$, which by several orders of magnitude exceeds the thermal energy at room temperature.

One also needs to be aware of the attractive van der Waals force, which can play a role for particles orbiting too close to the resonator surface. To estimate effects due to the van der Waals force, we use the estimate for the respective interaction energy between a dielectric sphere and a planar dielectric surface, which is suitable for the situation under consideration since $R_p \ll R_s$ [18]:

$$U_{VdW} \approx \frac{1}{6} \frac{H R_p}{r_0 - R_s - R_p}.$$

Here H is the Hamaker constant whose typical value can be taken to be $H \approx 10^{-19} J$. Assuming that the particle orbits the resonator at just about 10 nm above its surface, we obtain the estimate for $U_{VdW} \approx 10^{-18} J$. The energy associated with this force might have to be taken into account when designing the experiment, but should not preclude the orbital effect from being realized.

Actual observations of the predicted effects are facilitated by the fact that the dynamics of the particle is directly reflected in the properties of the electromagnetic field and can be observed optically. Figure 5 illustrates this point, showing time evolution of the surface field distribution of the resonator in its equatorial plane (as defined in the XYZ system). This field is strongly peaked along the axis connecting the center of the resonator and the particle [15,16]. In the regime under consideration here, the rotating particle drags this "hot" spot along, so that its spatiotemporal behavior directly reproduces the particle's trajectory and provides information about its angular frequency ζ/T. The flushes of intensity of the field along these trajectories reflect radial oscillations of the particle, while the decreasing intervals between consecutive maxima allow one to determine angular acceleration of the particle. Polar oscillations result in additional fluctuations of intensities with frequency different from that of radial oscillations and can, therefore, also be inferred from observation of the field.

V. CONCLUSION

In this paper, we demonstrate that confinement of the optical field in cavities significantly changes the nature of the optical forces exerted on small dielectric particles. We demonstrated

this point by rigorously calculating optical forces exerted by a spherical resonator on a small dielectric particle. The main qualitative prediction of the theory is that the nonconservative tangential component of the force in the high-Q resonators is proportional to the first order of the particle's static polarizability. This prediction can be verified by experimental observation of optically induced orbital motion of the particle in a moderately rarefied atmosphere. This result has important implications for the field of quantum cavity optomechanics, which is currently based on the assumption of the conservative nature of the cavity optical force. The developed theory also contributes to the field of optical biosensing by providing a theoretical framework for understanding the dynamic behavior of particles in typical biosensing experiments [3]. In addition, since dynamical aspects of particle behavior depend on their masses, the developed theory can be used as a foundation for optical mass sensing.

ACKNOWLEDGMENTS

The authors would like to thank S. Arnold for multiple illuminating discussions, and Queens College Research Enhancement Grant No. 90927-08-10 for partial financial support.

APPENDIX

Here we give a more detailed account of the derivation of various expressions presented in this work. The forces are obtained from electromagnetic fields outside of the resonator-particle system, which are found by applying the multisphere Mie approach [19] to the system of two spheres: one representing a resonator with radius R_s and refractive index n_s, and the other representing the particle with radius R_p and refractive index n_p. Both the particle and the resonator are assumed to be situated in a medium with refractive index n_0 and propagation constant $k = n_0\omega/c$, where ω is the driving frequency and c is the speed of light in vacuum. It is assumed that in the absence of the particle, an external field would excite a single fundamental WGM of the resonator with polar number $l = L$, polarization σ', frequency $\omega_L^{(0)}$, and width $\Gamma_L^{(0)}$.

1. VSH properties

A general monochromatic field can be expressed as a linear combination of vector spherical harmonics (VSHs) as

$$\mathbf{E} = E_0 e^{-i\omega t} \sum_{l=1}^{\infty} \sum_{m=-l}^{l} \sum_{\sigma=M,E} [C_{lm\sigma}\mathbf{H}_{lm\sigma}(\mathbf{r}) + P_{lm\sigma}\mathbf{J}_{lm\sigma}(\mathbf{r})], \tag{A1}$$

where $\mathbf{H}_{lm\sigma}$ and $\mathbf{J}_{lm\sigma}$ are vector spherical harmonics of the order of l,m and polarization $\sigma = E,M$. Defining $\mathbf{X}_{l,m} = -i\mathbf{r}\times\nabla Y_{lm}/\sqrt{l(l+1)}$ (where $Y_{l,m}$ is the scalar spherical harmonic), the magnetic (M) modes can be given as $\mathbf{J}_{lmM} = j_l(kr)\mathbf{X}_{l,m}$ and $\mathbf{H}_{lmM} = h_l^{(1)}(kr)\mathbf{X}_{l,m}$, where j_l and h_l are, respectively, the spherical Bessel function and spherical Hankel function of the first kind. The electric (E) modes are obtained by $\mathbf{J}_{lmE} = -i/k\nabla\times\mathbf{J}_{lmM}$ and $\mathbf{H}_{lmE} = -i/k\nabla\times\mathbf{H}_{lmM}$. Magnetic fields $\mathbf{H} = (-i/\omega\mu_0)\nabla\times\mathbf{E}$ (where μ_0 is the permeability of free space) are obtained by swapping polarizations on the coefficients in Eq. (A1), $[P, C_{lm(E,M)} \to P, C_{lm(M,E)}]$ and multiplying by $-i\sqrt{n_0\epsilon_0/\mu_0}$, where ϵ_0 is the permittivity of free space.

We use transformation properties of VSHs upon rotation defined by [19]

$$\mathbf{Z}_{lm\sigma}(\mathbf{r}') = \sum_{m=-l}^{l} D^l_{m'm}(\alpha,\beta,\gamma)\mathbf{Z}_{lm'\sigma}(\mathbf{r}), \tag{A2}$$

where $\mathbf{Z}_{lm\sigma}$ stands for $\mathbf{J}_{lm\sigma}$ or $\mathbf{H}_{lm\sigma}$, and $\mathbf{r}$ and $\mathbf{r}'$ denote the same point expressed in XYZ and $X'Y'Z'$, respectively, and $D^l_{m',m}$ is the Wigner D function. For $L \gg 1$, and in the vicinity of $\beta \approx -\pi/2$, we use the following approximate representation of $D^L_{m',L}$:

$$D^L_{m,L}(\alpha,\beta,\gamma) \approx \left(\prod_{n=0}^{m}\sqrt{\frac{L-n}{L+n}}\right)\frac{[\cot(\beta/2)]^m}{(\pi L)^{1/4}}\exp[-L(|\beta| - \pi/2)^2/2 - i\alpha m + i\gamma L + 1/8L]. \tag{A3}$$

The transformation of VSHs upon translation $\mathbf{r}' = \mathbf{r} + \mathbf{d}$ is given by the addition theorem [19],

$$\mathbf{Z}_{lmM}(\mathbf{r}') = \sum_{l'=1}^{\infty}\sum_{m'=-l'}^{l'}\left\{\mathcal{A}^{l,m}_{l',m'}(k,\mathbf{d})\tilde{\mathbf{Z}}_{l'm'M}(\mathbf{r}) + \mathcal{B}^{l,m}_{l',m'}(k,\mathbf{d})[i\tilde{\mathbf{Z}}_{l'm'E}(\mathbf{r})]\right\}, \tag{A4}$$

$$i\mathbf{Z}_{lmE}(\mathbf{r}') = \sum_{l'=1}^{\infty}\sum_{m'=-l'}^{l'}\left\{\mathcal{A}^{l,m}_{l',m'}(k,\mathbf{d})[i\tilde{\mathbf{Z}}_{l'm'E}(\mathbf{r})] + \mathcal{B}^{l,m}_{l',m'}(k,\mathbf{d})\tilde{\mathbf{Z}}_{l'm'M}(\mathbf{r})\right\}, \tag{A5}$$

where the tilde denotes $\mathbf{H}_{lm\sigma}$ for $|\mathbf{r}| > |\mathbf{d}|$ or $\mathbf{J}_{lm\sigma}$ for $|\mathbf{r}| < |\mathbf{d}|$. $\mathcal{A}^{l,m}_{l',m'}(k,\mathbf{d})$ and $\mathcal{B}^{l,m}_{l',m'}(k,\mathbf{d})$ are the so-called translation coefficients, which describe coupling between VSHs with different polar, azimuthal, and polarization indexes defined in shifted coordinate systems. The choice of the $X'Y'Z'$ coordinate system diagonalizes these coefficients with respect to the azimuthal indexes m and, since the VSH expansion of a dipole field contains only terms with $l = 1$, and $\sigma = E$, one of the polar and one of the polarization indexes in the translation coefficients are fixed at these values. Therefore, we can abridge notations for the translation coefficients keeping only three indexes referring to the mode of the resonator:

$$U_{lmE}(kr_p) = \mathcal{A}^{1,m}_{L,m}(k,r_p\hat{\mathbf{z}}') = (-1)^l\sqrt{\frac{3}{2}}\left[\sqrt{\frac{(l+1)(l+|m|)}{(2l+1)(|m|+1)}}h_{l-1}(kr_p) + (-1)^m \times\sqrt{\frac{2l(l+1)(l-|m|)+|m|l^2}{2(2l+1)}}h_{l+1}(kr_p)\right], \tag{A6}$$

$$U_{lmM}(kr_p) = \mathcal{B}^{1,m}_{L,m}(k,r_p\hat{\mathbf{z}}') = i(-1)^{l+1}\frac{\sqrt{3}}{2}m\sqrt{2l+1}h_l(kr_p), \tag{A7}$$

where r_p is the radial coordinate of the particle in the XYZ system and $\hat{\mathbf{z}}'$ is the unit vector along the Z' axes.

2. Field of the bisphere system

The field expansion coefficients [Eq. (A1)] for the stationary bisphere system are [16]

$$C_{lm\sigma} = \frac{D^L_{m,L}(\theta_p,\phi_p)}{\left[\alpha^{(1)}_{L\sigma_0}\right]^{-1} - \alpha^{(2)}_{1E}[U_{Lm\sigma_0}]^2} \times \begin{Bmatrix} 1 & l = L, \quad \sigma = \sigma_0 \\ \alpha^{(1)}_{l\sigma}\alpha^{(2)}_{1E}U_{Lm\sigma_0}U_{Lm\sigma} & \text{otherwise} \end{Bmatrix}, \quad \text{(A8)}$$

$$P_{lm\sigma} = \frac{D^L_{m,L}(\theta_p,\phi_p)}{\left[\alpha^{(1)}_{L\sigma_0}\right]^{-1} - \alpha^{(2)}_{1E}[U_{Lm\sigma_0}]^2}\alpha^{(2)}_{1E}U_{Lm\sigma_0}U_{Lm\sigma}, \quad \text{(A9)}$$

where θ_p and ϕ_p are the particle's angular coordinates in the XYZ system, and $D^L_{m,L}(\theta_p,\phi_p) \equiv D^L_{m,L}(\theta_p,\phi_p,0)$. Here we also use notation σ_0 to denote the polarization of the excited WGM. Quantities $\alpha^{(k)}_{l\sigma}$ are the Mie scattering coefficients for the resonator ($k = 1$) and the particle ($k = 2$). The former in the vicinity of a single WGM resonance can be presented as

$$\alpha^{(1)}_{l\sigma_0} = \delta_{l,L}\frac{-i\Gamma^{(0)}_L}{\omega - \omega^{(0)}_L + i\Gamma^{(0)}_L}, \quad \text{(A10)}$$

while the latter in the limit $nkR_p \ll 1$ is given by

$$\alpha^{(2)}_{1E} = -i\frac{2}{3}\frac{pk^3}{1 - \frac{2}{3}pk^3},$$

where

$$p = \frac{n^2-1}{n^2+2}(R_P)^3.$$

This quantity is related to the dipole polarizability of small particles (including radiation reaction) denoted in the main text as α:

$$\alpha = \frac{4\pi\epsilon_0 p}{1 - i(2/3)pk^3} \approx 4\pi\epsilon_0 p\left(1 + i\frac{2pk^3}{3}\right). \quad \text{(A11)}$$

The form of coefficients (A8) and (A9) indicate that the $2L - 2$ components of the initial WGM with $|m| > 1$ resonate at $\omega = \omega^{(0)}_L$, while the remaining $m = -1,0,1$ modes are shifted and broadened. The frequencies and widths for the $m = \pm 1$ modes, $\omega_p = \omega^{(0)}_L + \delta\omega_L$ and $\Gamma_p = \Gamma^{(0)}_L + \delta\Gamma_L$, are

$$\delta\omega_L = \frac{\mathrm{Re}[\alpha]k^3}{6\pi\epsilon_0}\Gamma^{(0)}_L[U_{L,1,\sigma_0}]^2, \quad \text{(A12)}$$

$$\delta\Gamma_L = \frac{2}{3}pk^3\delta\omega_L = \frac{\mathrm{Im}[\alpha]k^3}{6\pi\epsilon_0}\Gamma^{(0)}_L[U_{L,1,\sigma_0}]^2. \quad \text{(A13)}$$

The behavior of the $m = 0$ mode is polarization dependent. Its frequency and width, $\omega^\sigma_0 = \omega^{(0)}_L + \delta\omega^\sigma_L$, $\Gamma_\sigma = \Gamma^{(0)}_L + \delta\Gamma^\sigma_L$, are obtained by substituting $U_{L,0,\sigma_0}$ in place of $U_{L,1,\sigma_0}$ in (A12) and (A13). As $U_{L,0,M} = 0$, this resonance is only affected by the particle for E-polarized WGMs.

3. Equations of motion

The field and resulting forces are derived in the reference frame associated with the particle. In order to derive equations of motion for the particle, one needs to transform back to the stationary frame associated with the resonator. Generally speaking, in the case of a moving particle, this should involve the Lorentz transform of the fields. Since, however, the particle's motion is very slow, one can neglect all relativistic corrections including those resulting in the Doppler effect. In this case, the coordinate transformation involves simple vector rotation with a standard rotation matrix $\mathbf{A}$, such that $\mathbf{r} = \mathbf{A}^{-1}\mathbf{r}'$, and presents the dynamic equation as

$$md^2(\mathbf{A}^{-1}\mathbf{r}')/dt^2 = \mathbf{A}^{-1}\mathbf{F}',$$

where $\mathbf{F}'$ is the force calculated in the primed system and the particle's angular coordinates appear as elements of the rotation matrix. After introducing the dimensionless variables as explained in the main text, the equations of motion for the particle take the following form:

$$\frac{d^2y}{d\tau^2} = \frac{1+yb}{b}\left(\frac{d\bar{\theta}}{d\tau}\right)^2 + \frac{\zeta^2}{b(1+yb)^3} + \frac{F_r}{bf_0}, \quad \text{(A14)}$$

$$\frac{d\zeta}{d\tau} = \zeta\left(\frac{d\bar{\theta}}{d\tau}\right)\tan\bar{\theta} + (1+yb)\frac{F_\phi}{f_0}, \quad \text{(A15)}$$

$$\frac{d^2\bar{\theta}}{d\tau^2} = \frac{-2b}{1+yb}\left(\frac{dy}{d\tau}\right)\left(\frac{d\bar{\theta}}{d\tau}\right) - \frac{\zeta^2\tan\bar{\theta}}{(1+yb)^4} + \frac{1}{(1+yb)}\frac{F_\theta}{f_0}. \quad \text{(A16)}$$

Equations (10) and (11) are obtained by linearizing these expressions with respect to $\bar{\theta}$ and its time derivative, as well as by neglecting term yb in $1 + yb$.

[1] A. Ashkin, Phys. Rev. Lett. **24**, 156 (1970).

[2] M. Nieto-Vesperinas, P. Chaumet, and A. Rahmani, Philos. Trans. R. Soc. London A **362**, 719 (2004).

[3] S. Arnold, D. Keng, S. I. Shopova, S. Holler, W. Zurawsky, and F. Vollmer, Opt. Express **17**, 6230 (2009).

[4] J. Hu, S. Lin, L. C. Kimerling, and K. Crozier, Phys. Rev. A **82**, 053819 (2010).

[5] R. J. Schulze, C. Genes, and H. Ritsch, Phys. Rev. A **81**, 063820 (2010).

[6] D. E. Chang, C. A. Regal, S. B. Papp, D. J. Wilson, J. Ye, O. Painter, H. J. Kimble, and P. Zoller, Proc. Natl. Acad. Sci. **107**, 1005 (2010).

[7] O. Romero Isart, A. C. Pflanzer, M. L. Juan, R. Quidant, N. Kiesel, M. Aspelmeyer, and J. I. Cirac, Phys. Rev. A **83**, 013803 (2011).

[8] Z.-Q. Yin, T. Li, and M. Feng, Phys. Rev. A **83**, 013816 (2011).

[9] L. Landau, E. Lifshitz, and L. Pitaevskiĭ, *Electrodynamics of Continuous Media*, *Course of Theoretical Physics* (Butterworth-Heinemann, Oxford, 1984).

[10] A. Schliesser and T. J. Kippenberg, in *Advances In Atomic Molecular and Optical Physics*, edited by E. Arimondo, P. Berman, and C. C. Lin (Elsevier, New York, 2010), Vol. 58, pp. 207–323.
[11] A. Yang and D. Erickson, Lab Chip **10**, 769 (2010).
[12] H. Cai and A. W. Poon, Opt. Lett. **35**, 2855 (2010).
[13] M. Aspelmeyer, S. Groeblacher, K. Hammerer, and N. Kiesel, J. Opt. Soc. Am. B **27**, A189 (2010).
[14] A. Mazzei, S. Götzinger, L. de Menezes, G. Zumofen, O. Benson, and V. Sandoghdar, Phys. Rev. Lett. **99**, 173603 (2007).
[15] L. Deych and J. Rubin, Phys. Rev. A **80**, 061805 (2009).
[16] J. T. Rubin and L. Deych, Phys. Rev. A **81**, 053827 (2010).
[17] J. Chen, J. Ng, S. Liu, and Z. Lin, Phys. Rev. E **80**, 026607 (2009).
[18] B. Gady, D. Schleef, R. Reifenberger, D. Rimai, and L. P. DeMejo, Phys. Rev. B **53**, 8065 (1996).
[19] M. I. Mishchenko, L. D. Travis, and A. A. Lacis, *Scattering, Absorption and Emission of Light by Small Particles* (Cambridge University Press, Cambridge, 2002).